

Size Effects on Sheet-Metal Formability for Miniature Parts

Quang-Cherng Hsu

Department of Mechanical Engineering, National Kaohsiung University of Applied Sciences

415 Chien-Kung Rd., Kaohsiung 807, Taiwan, ROC.

hsuqc@cc.kuas.edu.tw

Keywords: Size effect, Sheet-metal forming, Miniature part, Strain analyzer, Stainless steel.

Abstract. Due to the rapid progress of industrial development, the formation of lightweight and small-size parts is becoming increasingly important. Especially in the IC and 3C industry, the sheet metal forming of miniature parts is especially interesting. Size effects such as specimen dimension, blank thickness, punch corner dimension, grain size, and grid dimension (for strain measurement), as well as the microstructure of material and surface condition all seriously influence the forming of miniature parts. In this paper, systematic experiments including Erichsen stretch forming and hydraulic bulge, and strain analyzers including for circular and rectangular grids are described for establishing the relationships of sheet metal formability to process parameters. The details of the experimental procedures and results are presented and discussed.

Introduction

Miniaturized parts and micro parts have become important in recent years due to the progress of the IC and 3C industries. When the feature size is between 10 and 1 mm, the specimen is in the miniaturized-parts category, in which parts can be produced by precision manufacturing process such as sheet-metal forming. Many processes related to miniaturized parts or microstructures have been successfully conducted by means of IC compatible processes [1].

Regarding micro forming, present information about IC compatible processes does not provide enough possibilities. Leopold [2] pointed out that the theoretical backgrounds related to micro forming are random theory of deformation, Monte-Carlo-method based nanoscale forming simulation, molecular dynamics analysis, rigid-plastic finite element analysis, and slip-line field theory based on a single-crystal forming model. Neugebauer [3] studied the superplastic embossing of a Zn-Al alloy. The results showed that micro forming behaviors are different from large-scale forming, which is obviously due to size effects.

Messner, Geiger and Tiesler [4-7] have conducted a series of micro-forming experiments, for example: tension tests, ring compression tests, and combined extrusion tests. Raulea [8] studied the relations between flow stress and the ratio of thickness to grain size by using uni-axial tension and simple bending tests. The results showed that yield strength decreases with a decreasing number of grains over the thickness up to one grain over the thickness; however, for grain sizes larger than the specimen thickness, the yield strength tends to increase with the increasing grain size. Picart [9] used a hydraulic bulging test for sheet-metal specimens to study the constitutive behavior. As seen in the above literature review, much research focuses on the size effects on the constitutive behavior as well as the material flow behavior, but provides little information on formability. In the present paper, systematic experiments are conducted for establishing the relationships of process parameters, specifically regarding size effects on formability.

Experimental methods

Fabrication Process of Fine Grids. The accuracy of the traditional electro-chemical etching processes for marking sunken grids is often affected by the accuracy of the electric wires in the template. Grids marked by using this method are often large, normally several mm. For example, for

the sheet metal used for car bodies, the grid dimensions are typically 2.54 mm in diameter and 2.85 mm in spacing as shown in Fig. 1(a). However, due to the need of micro sheet-metal forming for miniature parts, the accuracy of the above grids is not enough for strain analysis. The combination of photolithography and electro-chemical etching processes was used to mark fine grids with 0.4 mm in spacing, as shown in Fig. 1(b). Due to the restriction of photo-mask production, the above fine grids are square rather than circular. Combined photolithography and etching processes of marking fine grids on stainless steel surfaces are as follows: (1) cleaning the surface of the sheet metal; and spin coating the photo-resist on the surface to a thickness about 2.02 μm ; (2) placing a mask with square pattern of 34 μm in line width and 0.4 mm in spacing on the mask aligner; and using a UV lamp to irradiate the resist-coated sheet metal; (3) after development, the line width is about 34.19 μm ; and (4) using an electro-chemical etching process to produce etched grids 0.95 μm in depth and 31.17 μm in width; and cleaning the sheet-metal surface. This process is shown in Fig. 2.

Variation of Forming Dimensions. The hydraulic-bulging test was used to obtain plastic stress-strain relations because of its wide strain range before necking. The diameter of the stainless steel SUS304 specimen is 100 mm and its thicknesses are 0.8, 0.6, and 0.3 mm. To evaluate the size effects on formability, three punch diameters were studied: 50, 20 and 10 mm. Two surface conditions with dry friction were also studied, marked as 2B (diffuse surface) and BA (shiny surface).

Strain analyzer. A strain analyzer system for coarse circular grid developed by the author [10] was used in this work to measure forming-limit strains. Figure 3 depicts the strain measurement of coarse circular grids. In order to obtain a reasonable limit strain range, one must identify a symmetric line of crack region. Then a cracked grid and an uncracked grid near this line were measured.

If a square grid is used, the strain calculation can be based on two triangular grids (i.e. halves of the square grid). Assume that the deformation is linear within this grid, no shear strain occurs outside the plane, and axes of X and Y coincided with two different sides of triangle grid are chosen, as shown in Fig. 4. Therefore, the strains can be calculated based on the stretch ratio and angle change of these two sides (ab and ac change into $a'b'$ and $a'c'$) [11]. The relation of Green deformation tensor C and stretch ratio ds/dS (the ratio of deformed length to original length) is represented as

$$\left[\frac{ds}{dS} \right]^2 = N'CN, \quad (1)$$

where N is a unit vector along the dS direction and N' is its transport. Due to the relation of Lagrangian strain tensor E and Green deformation tensor C , the following equation can be obtained:

$$\begin{aligned} E_{11} &= \frac{(x_2 - x_1)^2 + (y_2 - y_1)^2 + (z_2 - z_1)^2 - D^2}{2D^2} \\ E_{22} &= \frac{(x_3 - x_1)^2 + (y_3 - y_1)^2 + (z_3 - z_1)^2 - D^2}{2D^2} \\ E_{12} &= E_{21} = [(x_2 - x_1)(x_3 - x_1) + (y_2 - y_1)(y_3 - y_1) + (z_2 - z_1)(z_3 - z_1)] / (2D^2). \end{aligned} \quad (2)$$

The principal strains can be represented as:

$$E_{1,2} = \frac{E_{11} + E_{22}}{2} \pm \sqrt{\left(\frac{E_{11} - E_{22}}{2} \right)^2 + E_{12}^2}. \quad (3)$$

Due to the relation of stretch ratio and principal strain, the natural strains can be represented as:

$$\varepsilon_{1,2} = \ln\left(\frac{l}{l_0}\right) = \ln\sqrt{1 + 2E_{1,2}}. \quad (4)$$

Figure 5 depicts the strain measurement of fine square grids. As the same reason of coarse-grid measurement in Fig. 3, one must identify a symmetric line of crack region. Then a cracked grid and an uncracked grid near this line were measured.

Results and Discussion

Three specimens with the same experimental conditions (i.e. the same surface quality, thickness, specimen size, grid size, and punch diameter) were pressed. The forming limit strain of each specimen was measured based on at least two different grids that are close to the crack region (i.e. the cracked grids and the uncracked grids both in Figs. 3 and 5). The experimental results are shown in Table 1. The standard deviation of the forming-limit strain is about 0.015.

Surface-condition Effect on Formability. Due to friction traction between the specimen surface and the punch surface in the Erichsen test, the strain state of stretch forming is close to plane-strain forming; that is the minor strain is very close to zero. Therefore, only a discussion of formability is considered in major strain. Two kinds of surface condition (2B and BA) are used to study surface condition effects on formability. A Tencor Alpha Step 500 profile meter was used to measure the surface roughness of the two surfaces, as shown in Table 2. Although the formability of the shiny surface is a little larger than that of the diffuse surface, there is no significant difference, as shown in Table 3. Although it might be expected that the smoother surface would be more formable than a slightly roughed surface, on a molecular scale, the small differences between the two surfaces are still important enough to study in detail in future.

Punch Size Effect on Formability. From Table 1, under the same thickness condition and the same etching grid, if the punch size changes from $\phi 50$ to $\phi 20$, then the major strain reduces and the minor strains increase. This means that the strain path changes when the punch size changes, as shown in Fig. 6 and 7.

Grid Size Effect and Thickness Size Effect on Formability. Table 1 shows that, under the same thickness conditions, the formability measured when etching fine grids on the sheet-metal surface is better than etching coarse grids. Comparing Fig. 6 and 7 reveals the same conclusion. This is because smaller grids can reveal cracking regions more precisely than larger grids. However, etching small grids is a more complicated process and is more expensive. Figure 8 demonstrates the measured formability when etching three different spacings of grid: 2.85 mm, 2.54 mm and 0.4 mm on sheet-metal surface of 0.3 mm thickness. The smaller the grids were etched on metal surface, the larger formability could be obtained. In Fig. 6 and 7 also show that formability of thick metal is better than that of thin metal.

Conclusions

Studies of the punch formability of type 304 stainless steel have resulted in the following conclusions: (1) As material thickness is increased, the forming-limit strain also increases, but the ratio is not proportional; (2) In measuring forming-limit strain, fine grid patterns give superior accuracies than coarse grids; (3) When the punch diameter is reduced, the major-limit strain decreases while the minor-limit strain increases.

Experimental studies show that, when forming miniature parts, formability need to be re-evaluated. Fine grid must be used instead of coarse grid in order to obtain enough accuracy. For fine grid etching techniques, the combined photolithography and electro-chemical etching processes is proposed. When using a fine grid to measure formability, the results are bigger and better than using coarse grids.

This is because fine grids can reach cracking region more closely than coarse grids. However, etching finer grids entails more complicated processes and therefore is more expansive.

Acknowledgments

The author would like to acknowledge the financial support of National Science Council under Grant No. NSC 89-2212-E151-023.

References

- [1] Madou, M., *Fundamentals of Microfabrication*. (CRC Press, New York, 1997).
- [2] Leopold, J., Foundations of Micro – Forming, Advanced Technology of Plasticity, Proc. 6th ICTP, Nuremberg, Germany, **II**, 883 (1999).
- [3] Neugebauer, R., et al., High Precision Embossing of Microparts, Advanced Technology of Plasticity, Proc. 6th ICTP, Nuremberg, Germany, **II**, 921 (1999).
- [4] Messner, A., et al., Size effect in the FE-simulation of micro-forming process, J. Mat. Pro. Technol. **45**, 371 (1994).
- [5] Geiger, M., et al., Metal forming of micro parts for electronics, Production Engineering, **II (1)**, 15 (1994).
- [6] Geiger, M., et al., Design of micro-forming processes – fundamentals, material data and friction behaviour,” Proc. 9th Int. Cold Forging Congress, Solihull, UK. 155 (1995).
- [7] Tiesler, N., Engel, U. and Geiger M., Forming of microparts – effects of miniaturization of friction, Advanced Technology of Plasticity, Proc. 6th ICTP, Nuremberg, Germany. **II**, 889 (1999).
- [8] Raulea, L. V., Govaert, L. E. and Baujjeus, F. P. T., Grain and specimen size effects in processing metal sheets,” Advanced Technology of Plasticity, Proc. 6th ICTP, Nuremberg, Germany. **II**, 939 (1999).
- [9] P. Picart, J. F. Michel, Effects of size and texture of the constitutive behaviour for very small components in sheet metal forming,” Advanced Technology of Plasticity, Proc. 6th ICTP, Nuremberg, Germany. **II**, 895 (1999).
- [10] Hsu, Q. C., Comparison of different analysis models to measure plastic strains on sheet metal forming parts by digital image processing, Int. J. Mach. Tools & Manuf. **43**, 515 (2003).
- [11] Malvern, L. E., *Introduction to the Mechanics of a Continuous Medium*, Prentice-Hall, New Jersey (1969).

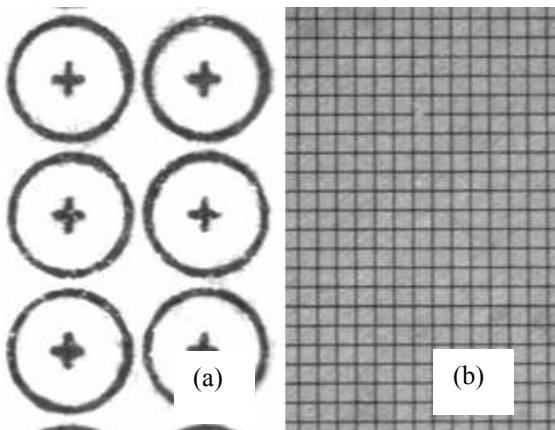


Fig. 1. Grid patterns for strain measurement. (a) Coarse grids (2.54 mm in diameter and 2.85 mm in spacing), (b) Fine grids (0.034 mm in width and 0.4 mm in spacing).

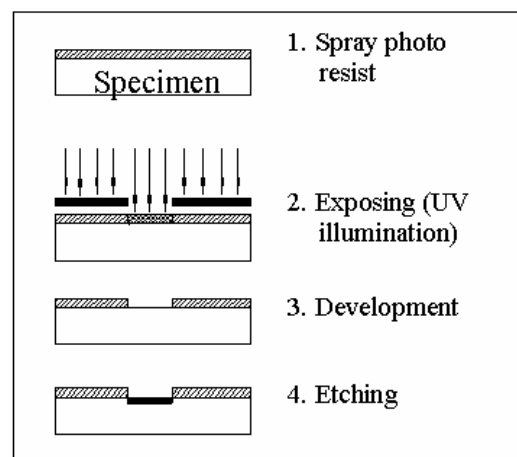


Fig. 2. Combined photolithography and etching processes for applying fine grids to a stainless steel surface.

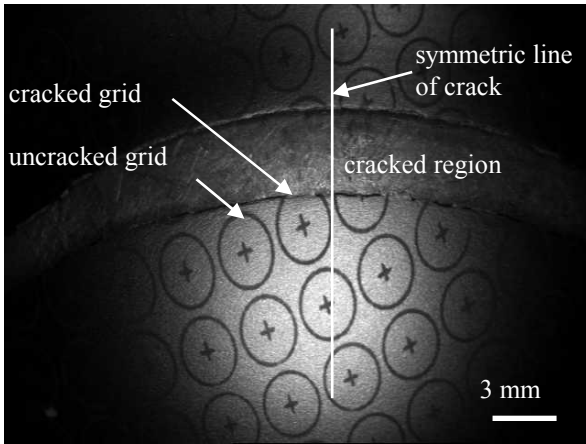


Fig. 3. Strain measurement of coarse circular grids ($\phi 2.54$ mm).

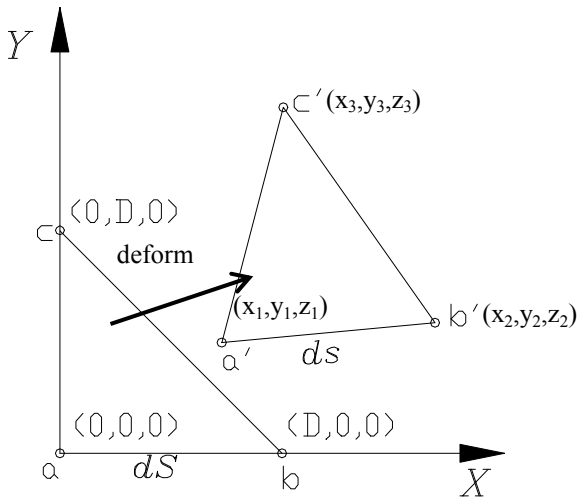


Fig. 4. Triangle grids before and after deformation.

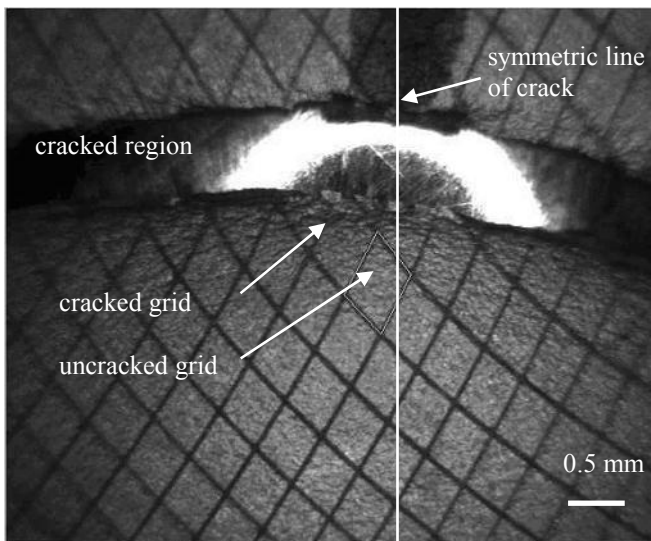


Fig. 5. Strain measurement of fine square grids ($\square 0.4$ mm).

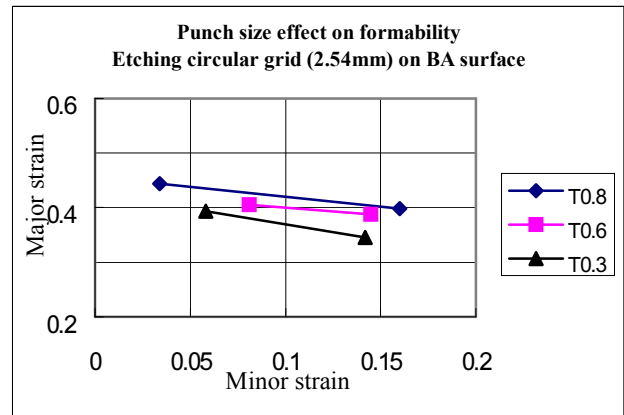


Fig. 6. The punch-size effect on formability (in each line, the left point represents the $\phi 50$ punch; the right point represents the $\phi 20$ punch).

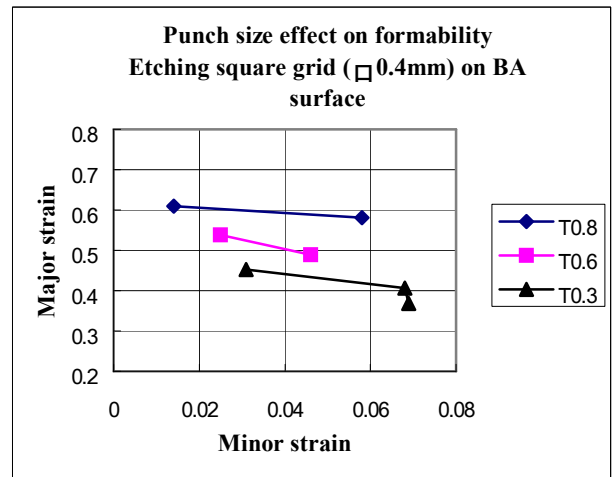


Fig. 7. The punch size effect on formability (in each line, the left point represents the $\phi 50$ punch; the right point represents the $\phi 20$ punch).

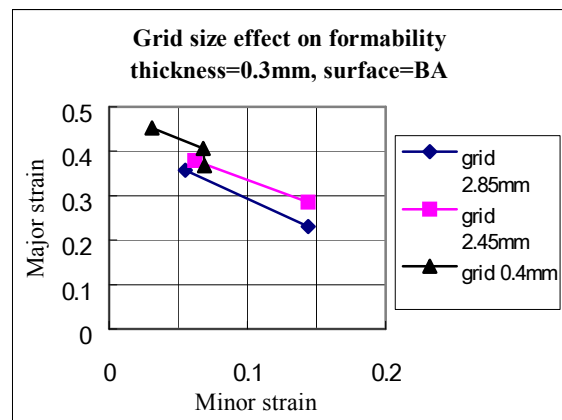


Fig. 8. Formability when etching three different kinds of grids: 2.85 mm, 2.54 mm and 0.4mm (in each line, left point represents $\phi 50$ punch; right point represents $\phi 20$ punch).

Table 1. Forming limit strain of stretch forming.

Grid Patterns and dimensions	Punch diameter, Thickness (mm)	2B (diffuse surface)				BA (shiny surface)			
		uncracked grid		cracked grid		uncracked grid		cracked grid	
		ε_1	ε_2	ε_1	ε_2	ε_1	ε_2	ε_1	ε_2
Circular grid $\phi 2.54\text{mm}$	$\phi 50$ T0.8	0.445	0.053	0.463	0.054	0.444	0.034	0.491	0.042
	$\phi 20$ T0.8	0.388	0.153	0.419	0.143	0.398	0.160	0.423	0.159
	$\phi 50$ T0.6	0.428	0.07	0.419	0.067	0.405	0.081	0.419	0.073
	$\phi 20$ T0.6	0.385	0.134	0.414	0.137	0.388	0.145	0.401	0.155
	$\phi 50$ T0.3	0.379	0.056	0.409	0.052	0.393	0.058	0.413	0.064
	$\phi 20$ T0.3	0.354	0.136	0.366	0.139	0.346	0.142	0.373	0.142
Square grid $\square 0.4\text{mm}$	$\phi 50$ T0.8	0.607	0.027	0.608	0.025	0.610	0.014	0.640	0.014
	$\phi 20$ T0.8	0.547	0.070	0.588	0.064	0.581	0.058	0.588	0.070
	$\phi 50$ T0.6	0.536	0.052	0.554	0.024	0.538	0.025	0.562	0.042
	$\phi 20$ T0.6	0.527	0.044	0.571	0.042	0.489	0.046	0.513	0.049
	$\phi 50$ T0.3	0.465	0.035	0.492	0.043	0.452	0.031	0.473	0.025
	$\phi 20$ T0.3	0.393	0.050	0.441	0.048	0.407	0.068	0.429	0.068
	$\phi 10$ T0.3	0.380	0.060	0.410	0.061	0.368	0.069	0.398	0.069

Table 2. Surface roughness of three different thickness metals.

Thickness (mm)	Surface roughness on 2B (diffuse surface)		Surface roughness on BA (shiny surface)	
	Parallel direction	Perpendicular direction	Parallel direction	Perpendicular direction
T0.8	645.85(Å)	1203.7(Å)	284.96(Å)	280.10(Å)
T0.6	500.55(Å)	618.23(Å)	152.95(Å)	292.53(Å)
T0.3	557.97(Å)	819.98(Å)	225.67(Å)	317.83(Å)

Table 3. Forming limit strains based on different grid patterns and punch diameters but the same thicknesses.

Grid pattern and dimension	Punch diameter, thickness (mm)	2B (diffuse surface)				BA (shiny surface)			
		uncracked grid		cracked grid		uncracked grid		cracked grid	
		ε_1	ε_2	ε_1	ε_2	ε_1	ε_2	ε_1	ε_2
Square $\square 2.85\text{mm}$	$\phi 50$ T0.3	0.329	0.061	0.366	0.057	0.358	0.055	0.386	0.053
	$\phi 20$ T0.3	0.278	0.147	0.303	0.153	0.231	0.144	0.310	0.145
Circular $\phi 2.54\text{mm}$	$\phi 50$ T0.3	0.570	0.063	0.392	0.060	0.379	0.062	0.394	0.055
	$\phi 20$ T0.3	0.288	0.127	0.336	0.139	0.285	0.144	0.323	0.123
Square $\square 0.4\text{mm}$	$\phi 50$ T0.3	0.465	0.035	0.492	0.043	0.452	0.031	0.473	0.025
	$\phi 20$ T0.3	0.393	0.050	0.441	0.048	0.407	0.068	0.429	0.068
	$\phi 10$ T0.3	0.380	0.060	0.410	0.061	0.368	0.069	0.398	0.069

Progress on Advanced Manufacture for Micro/Nano Technology 2005

doi:10.4028/www.scientific.net/MSF.505-507

Size Effects on Sheet-Metal Formability for Miniature Parts

doi:10.4028/www.scientific.net/MSF.505-507.721